ICASSP 2024 - 2024 IEEE International Conference on Acoustics, Speech and Signal Processing (ICASSP), Seoul, Korea, Republic of. April 2024
Pages 8711-8715
https://doi.org/10.1109/ICASSP48485.2024.10446834
https://archimer.ifremer.fr/doc/00885/99670/

Deep Learning Inversion of Ocean Wave Spectrum from SAR Satellite Observations

Tripathi S.P. [1], Chapron Bertrand [3], Collard F. [2], Guitton Gilles [2], Lopez-Radcenco Manuel [2], Mouche Alexis [3], Fablet Ronan [1]

[1] IMT Atlantique, UMR CNRS Lab-STICC, Brest, FRANCE
[2] OceanDataLab, Locmaria-Plouzane, FRANCE
[3] Ifremer, LOPS, Brest, FRANCE

Abstract :

The monitoring of waves at the ocean surface is critical for both operational needs (e.g., maritime traffic) and scientific studies (e.g., air-sea interactions). Synthetic aperture radar (SAR) Satellites provide one of the only remote sensing observations to retrieve ocean wave information on a global scale. However state-of-the-art SAR processing schemes often lead to poor inversion performance due to overly-simplistic assumptions. Here we leverage deep learning schemes to address these shortcomings. We state the targeted measurement of the ocean wave spectrum at sea surface as a neural mapping from SAR satellite observations. We exploit supervised deep learning schemes trained from a large-scale collocation dataset between real SAR observations and Wavewatch III model data. Our results emphasize for the first time how deep learning schemes can outperform the state-of-the-art analytical SAR-based inversion with an improvement in terms of mean square error greater than 65%. We analyse and discuss further the key features of the trained neural processing.

Keywords : Deep learning, SAR imagery, Ocean remote sensing, Wave spectrum, Inverse problem

1. INTRODUCTION

The monitoring of ocean waves at the ocean surface is critical for both operational needs (e.g., maritime traffic) and scientific studies (e.g., air-sea interactions) [2][3]. In this context, the retrieval of ocean wave spectra is a key challenge. It informs us on the frequency-direction distribution of sea surface waves at any space-time location. While moored observatories deliver a direct measurement of these wave spectra, they involve a very scarse spatial sampling. As such, they cannot deliver a synoptic view of ocean wave dynamics on a global scale. Numerical models such as WaveWatch III (WW3) [4] [5]provide means to solve sampling gaps. They may however involve significant uncertainties [6]. Especially, they cannot account for fine-scale variabilities and complex air-sea and wave-current interactions [6].

Satellite ocean remote sensing provides means to monitor the sea surface from space. In particular, synthetic aperture radar (SAR) imagery provides through the signal backscattered by the sea surface an indirect observation of the sea surface state, including among others wind, rain and wave signatures [1]. The complexity of the SAR process as well as of the non-linear interactions between the backscattering and the sea surface state make the inversion of the SAR observation highly challenging. For instance, the cutoff phenomenon prevents the SAR process to actually image large wave numbers in the azimuthal direction . This results in a poor reliability of analytical model-driven inversion schemes as they cannot account for such non-linear patterns [7], as illustrated in Fig.1.

Deep learning has emerged as a powerful paradigm to address inversion problems as the supervised learning of an inverse operator from training data [8]. Numerous remote sensing studies have recently leveraged this approach [9], including for satellite SAR observations [10]. Regarding sea surface waves, deep learning schemes have significantly improved the retrieval of significant wave height from SAR observations [11]. The significant wave height is an average quantity, which derives from the total energy of the wave spectrum.

This paper explores further deep learning schemes for the inversion of SAR observations of the sea surface. We address the retrieval of the entire wave spectrum. Our contribution lies both in the collection of a large-scale collocated datasets of SAR sea surface observations and WW3 data and in the development of supervised deep learning schemes. We propose different neural architectures. Our numerical experiments support their relevance to outperform the baseline approach and address the complexity of the SAR processing.

This paper is organized as follows. Section 2 introduces related background. We describe the proposed approach in Section 3 and detail our numerical experiments in Section 4. Section 5 discusses our main contributions.

2. PROBLEM STATEMENT

Through the signal backscattered by the sea surface, satellite SAR sensors can image the energy of sea surface waves

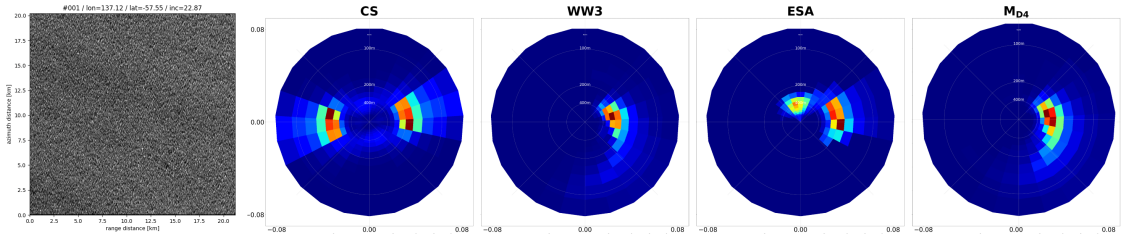

Fig. 1: **Inversion of the sea surface wave spectrum from a Sentinel-1 SAR observation:** from left to right, SAR roughness image, magnitude of the SAR cross-spectrum, collocated WW3 wave spectrum used as reference data, state-of-the-art analytical SAR-based inversion [1], proposed learning-based inversion. We depict all spectra as normalized spectra using the same colorbar.

and their frequency-direction distribution [12]. The SAR processing relies on the analysis of different looks through cross-spectra [1]. But, it only directly informs the energy that is at azimuthal wave numbers below the cutoff value and at range wave numbers smaller than the spatial resolution of the sensor by the SAR process. The cutoff phenomenon then affects the SAR imaging process in high waves conditions. It results in a displacement and loss of the energy in the azimuth direction of the satellite. This effect can impact entire wave systems if they are at not at low enough azimuthal wave numbers.

This SAR imaging process transfers into a complex non-linear and possibly non-bijective function to map SAR-derived signatures, such as the SAR cross spectrum, to wave spectrum. These issues have plagued analytical inversion approaches. The state-of-the-art inversion scheme [1] cannot retrieve any wave spectrum information above the cutoff. Besides, the considered over-simplifying assumptions may even result in artifacts through dubious high-energy patterns as illustrated in Fig.1. The analytical baseline retrieves a high-energy wave pattern northwards for northward wavenumbers between 0.05 rad.m^{-1} and 0.2 rad.m^{-1}. This directly relates to the inability of lifting the directional uncertainty as evidenced by the weak consistency with the WW3 data.

Recently, deep learning has emerged as an appealing framework for SAR-based ocean remote sensing [13], including for the estimation of the significant wave height of the ocean from SAR cross spectra [11]. As the significant wave height relates to the total energy of the wave spectrum, these results support the ability of deep learning to retrieve relevant features of all wave systems, including beyond the cutoff value, from partial SAR-derived features.

Here, we aim to explore further how deep learning can reveal the potential of SAR sea surface observations to monitor sea surface wave dynamics, in particular their frequency-direction distribution.

3. PROPOSED APPROACH

This section presents the proposed deep learning approach for the inversion of ocean wave spectrum from SAR observations. It relies on the supervised learning of a mapping between SAR-derived cross-spectrum and the normalized frequency-direction wave spectrum. We first introduce the data collection process to build a large-scale training dataset. We then present the considered deep neural schemes.

3.1. Collocated Datasets

To our knowledge, we provide the first reference dataset to address the learning-based inversion of sea wave spectrum from SAR observations. Due to the limited availability of in situ data, especially in terms of spatial coverage of the global ocean, we exploit collocations between Sentinel-1 SAR observations and the hindcasts of the WW3 model over a whole year, namely 2020. We use the latter as the groundtruth data for the wave spectrum. These hindcasts show a good average match to in situ observation datasets [5][6]. They were also used as reference data for the training of deep learning schemes for the estimation of the significant weight height. We may however point out that these hindcasts are only an estimation of the real wave distribution. As such, they involve uncertainties to be accounted for in our analysis. Overall, we consider a polar grid for the discretization of the frequency-direction domain with 24 wavenumbers from 0.005 rad.m^{-1} to 2.063 rad.m^{-1} and 32 angular bins from 0° to 345°.

From previous numerical experiments, we noted that the available ESA Level-2 data of sentinel-1 SAR data and the associated cross-spectrum data, referred to as the Quality cross spectrum dataset, involved complex noise patterns due to the considered non-linear processing. We then chose to recompute raw cross spectrum from the 3 individual looks of each sentinel-1 SAR Image. We use the resulting average absolute and imaginary cross spectra as our SAR-derived dataset. We re-interpolate all cross-spectra on the same North-based polar grid as WW3 wave spectrum data.

We complement the resulting collocated dataset with the SAR cross-spectrum simulated from the WW3 wave spectrum using a closed-form solution [14]. We also include the ESA OCN Level 2 Wave spectrum (ESA-WS) product. This product relies on an analytical model-based inversion [15][1][12]. It provides the state-of-the-art operational base-

line for benchmarking purposes. Overall, our dataset comprises 142000 samples. We focus on normalized spectra to address the frequency-direction distribution patterns such that each sample of the dataset combines: (i) a normalized SAR cross spectra referred to as CS of shape $(n, 2, 24, 32)$, (ii) a normalized WW3 wave spectra referred to as $WW3$ of shape $(n, 24, 32)$, (iii) a normalized Simulated SAR cross spectra referred to as CF of shape $(n, 2, 24, 32)$, (iv) a normalized ESA OCN Level 2 wave spectra referred to as ESA of shape $(n, 24, 32)$ with n the number of samples. We randomly pick 100000 samples to create a training dataset and 10000 samples for the validation dataset. The remaining ones form the test dataset.

3.2. Neural architecture(s)

The targeted problem can be regarded as the learning of a mapping from two-dimensional tensors to two-dimensional tensors using polar coordinates. Image-to-image neural architectures naturally apply. Following numerous studies which support the relevance of U-Nets [16] to solve inverse problems in computational imaging [17], we choose a U-Net as our baseline neural architecture. We may emphasize that we expect the targeted SAR inversion problem to require a non-local analysis. Through the implemented scale-space decomposition, the U-Net provides means to account for this important feature. By contrast, a simple ConvNet [18] seems less appropriate as supported by preliminary experiments. Besides this direct U-Net-based inversion scheme, we investigate a second type of architecture, which explicitly benefit from the availability of a closed form to simulate SAR cross-spectrum from wave spectrum. We decompose the inversion scheme as a series of 2 U-Net: the first one aiming at pre-processing and denoising the SAR cross-spectrum and the second one solving the inverse problem for the analytical simulation of SAR cross-spectrum from wave spectrum. Compared with the baseline U-Net architecture, this second architecture offers a greater interpretability, especially to characterize and understand the information extraction step from real SAR observations. For both types of architectures, the input shape of the network is $(2, 24, 32)$ and the output shape $(1, 24, 32)$. Regarding the parametrization of the U-Net, we vary the numbers of encoding-decoding layers from 1 to 4 and perform a sensitivity analysis. Let us denote by M_{Dj} the first U-Net model with j the number of encoding-decoding layers, by M_{PP4} and M_{I4} the pre-processing[1] and inversion U-Net for the second architecture.

3.3. Learning scheme and implementation aspects

As training loss for the direct inversion scheme, we consider the mean-square error (MSE) of the output of our model and $WW3$ as follows:

$$\mathcal{L}(Z, WW3) = \frac{\lambda_{\text{D}}}{N} \sum_{i=0}^{N} \|Z_i - WW3_i\|^2 \quad (1)$$

$\lambda_{\text{D}} = 1000$, $Z = M_{\text{D}}(CS)$ and N the batch size

Regarding the two-stage architecture, the training loss combines a pre-processing loss based on the MSE between output of the pre-processing block and the SAR cross-spectrum simulated from the WW3 wave spectrum, and an inversion loss based on the MSE between the output of the inversion block and the WW3 wave spectrum. This leads to the definition of the loss following:

$$\mathcal{L} = \frac{1}{N} \sum_{j=0}^{N} (\lambda_{\text{I}} \|Z_j - WW3_j\|^2 + \lambda_{\text{PP}} \|Y_j - CF_j\|^2) \quad (2)$$

$\lambda_{\text{I}} = 1000, \lambda_{\text{PP}} = 100$, $Y = M_{\text{PP}}(CS)$, $Z = M_{\text{I}}(Y)$ and N the batch size

In both experiments, we use the Adam Optimizer with a learning rate of $5 * 10^{-4}$ and a batch size of 100. The repository with our source code and all the experiments is available on: https://github.com/CIA-Oceanix/SAR-Based-Wave-inversion. In terms of computational complexity, our direct inversion model and our two-stage scheme involve respectively about 7.7M and 15.4M parameters.

4. RESULTS

Metrics	MSE	Bias	Corr Coeff
ESA	**7.16**	**0.03**	**0.56**
M_{D1}	3.56 $\pm$ 0.06	0.01$\pm$ 0.01	0.65 $\pm$ 0.03
M_{D2}	2.94 $\pm$ 0.04	0.02 $\pm$ 0.01	0.77 $\pm$ 0.04
M_{D3}	2.65 $\pm$ 0.03	0.01 $\pm$ 0.01	0.80 $\pm$ 0.03
M_{D4}	**2.52 $\pm$ 0.04**	**0.02 $\pm$ 0.01**	**0.83 $\pm$ 0.02**
$M_{\text{PP4}} + M_{\text{I4}}$	**2.53 $\pm$ 0.03**	**0.02 $\pm$ 0.01**	**0.83 $\pm$ 0.03**

Table 1: Benchmarking of the proposed learning-based schemes with regards to the baseline state of the art [1]

We report our numerical experiments to benchmark the proposed learning-based inversion schemes with respect to the state-of-the-art ESA processing [15][19]. In Table 1 we report three performance metrics evaluated on the test dataset: namely the MSE, the associated mean bias and the correlation score between the reconstructed wave spectrum and the WW3 reference. Besides the ESA processing baseline, we assess the performance of a direct U-net-based inversion with 1 to 4 encoding-decoding layers and of the two-stage architecture. All learning-based models clearly outperform the baseline with a reduction of the MSE by 50% or more. The best two models with a very similar performance are the

[1]The pre-processing is meant to include a denoising of the spectrum but also to account for other complex features of SAR observations

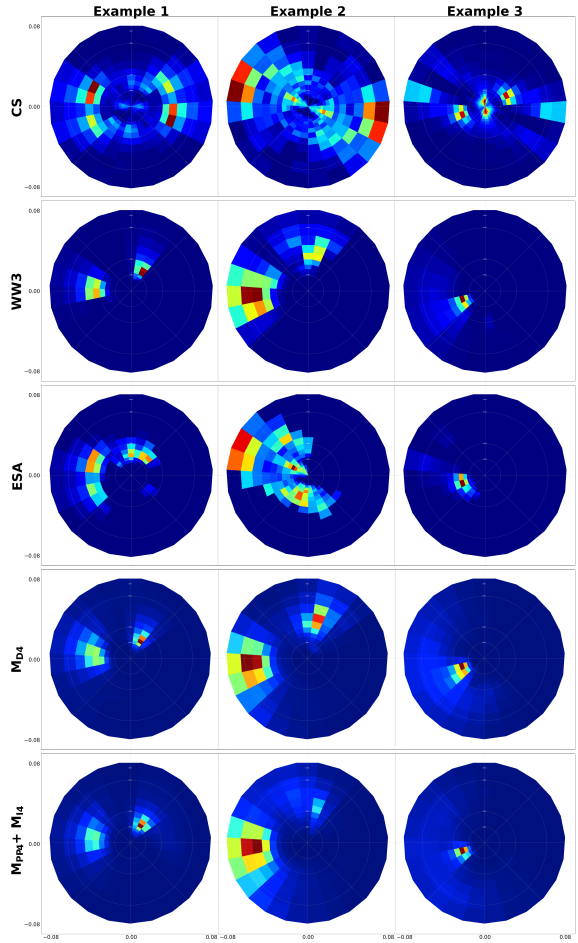

(a) **Inversion of the sea surface wave spectra from three Sentinel-1 SAR observation:** magnitude of the SAR cross-spectrum, collocated WW3 wave spectrum used as reference data, state-of-the-art analytical SAR-based inversion [1], M_{D4} inversion, M_{PP4}+M_{I4} inversion. We depict all spectra as normalized spectra using the same colorbar.

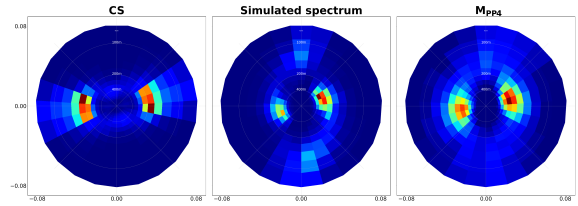

(b) **Reconstruction of a WW3-based simulated cross-spectrum[14] from corresponding Sentinel-1 SAR observation:** magnitude of the SAR cross-spectrum, simulated cross-spectrum, M_{PP4} reconstruction. We depict all spectra as normalized spectra using the same colorbar

Fig. 2

direct U-Net inversion with 4 encoding-decoding layers and the two-stage inversion schemes. They both outperform the ESA baseline by more than 65% in terms of MSE and by more than 50% in terms of correlation coefficient. These experiments also clearly stress the relevance of the multi-scale processing performed by U-Nets. The 4-scale configuration (M_{D4}) improves by 30% the MSE score of the single-scale configuration, which resorts to a simple CNN. We report in Fig.1 and Fig.2a inversion examples with a comparison between the input SAR cross-spectrum, the WW3 wave spectrum reference and the reconstructed wave spectrum using the ESA baseline, U-Net scheme M_{D4} and the two-stage architecture M_{PP4}+M_{I4}. These examples involve high cutoff conditions. We clearly see that the inversion of the SAR cross-spectrum is not a simple denoising problem to retrieve the wave spectrum. The difference between the WW3 reference and ESA baseline further illustrates the complexity of the inversion problem. Especially, the cutoff phenomenon leads to large directional errors for the ESA baseline. By contrast, the learning-based scheme relevantly retrieve the different high-energy wave patterns. This is particularly illustrated in Fig.1 where the baseline estimate a northward energy partition that is actually only the continuity of the main partition in the opposite direction. We observe a similar behaviour in the second example displayed in Fig.2a. The ESA model assigns the energy southward while it should form a northward partition as correctly retrieved by the learning-based schemes. We also observe a better performance in the area which is not affected by the cut-off phenomenon. The learning-based schemes retrieve wave spectra closer to the WW3 reference and show some robustness to the noise and artifacts present in the SAR cross-spectra. As stated before, M_{D4} and M_{PP4}+M_{I4} schemes lead to very similar results. Beyond the inspection of the agreement between the reconstructed and reference wave spectra illustrated in Fig.2b, we can also analyze the agreement between the pre-processed SAR cross-spectrum, *i.e.* the output of the first stage M_{PP4}, and the SAR cross-spectrum simulated from the WW3 wave spectrum. It highlights the ability of the two-stage architecture to retrieve energy patterns above the cutoff in the SAR cross-spectra so that the inversion is consistent with the wave-spectrum-to-SAR simulation model. While sharing the same global patterns in the example depicted in Fig.2a, the pre-processed and WW3-derived SAR cross-spectrum also show some differences. The learning process may result in some over-smoothing of some structures but some differences in the intensity and spread of the observed structures may also relate to the differences between the true sea state and the WW3 prediction.

5. CONCLUSION

We have investigated how deep learning methods can solve the inversion of the sea surface wave from satellite-derived SAR observations. Using collocated SAR data and model-based wave spectrum data, we have developed a supervised scheme and have demonstrated its potential to largely outperform operational analytical methods and address intrinsic issues of SAR imaging. Future work will investigate its application to in-situ sea state measurements.

6. REFERENCES

[1] G. Engen and H. Johnsen, "Sar-ocean wave inversion using image cross spectra," *IEEE Transactions on Geoscience and Remote Sensing*, vol. 33, no. 4, pp. 1047–1056, 1995.

[2] Alex Ayet and Bertrand Chapron, "The dynamical coupling of wind-waves and atmospheric turbulence: a review of theoretical and phenomenological models," *Boundary-Layer Meteorology*, vol. 183, no. 1, pp. 1–33, 2022.

[3] Michael L. Banner, "The influence of wave breaking on the surface pressure distribution in wind—wave interactions," *Journal of Fluid Mechanics*, vol. 211, pp. 463–495, 1990.

[4] Hendrik L Tolman et al., "User manual and system documentation of wavewatch iii tm version 3.14," *Technical note, MMAB Contribution*, vol. 276, no. 220, 2009.

[5] Qingxiang Liu, W Erick Rogers, Alexander V Babanin, Ian R Young, Leonel Romero, Stefan Zieger, Fangli Qiao, and Changlong Guan, "Observation-based source terms in the third-generation wave model wavewatch iii: Updates and verification," *Journal of Physical Oceanography*, vol. 49, no. 2, pp. 489–517, 2019.

[6] Fan Bi, Jinbao Song, Kejian Wu, and Yao Xu, "Evaluation of the simulation capability of the wavewatch iii model for pacific ocean wave," *Acta Oceanologica Sinica*, vol. 34, pp. 43–57, 2015.

[7] Xuan Wang, Romain Husson, Haoyu Jiang, Ge Chen, and Guoping Gao, "Evaluation on the capability of revealing ocean swells from sentinel-1a wave spectra measurements," *Journal of Atmospheric and Oceanic Technology*, vol. 37, no. 7, pp. 1289 – 1304, 2020.

[8] Alice Lucas, Michael Iliadis, Rafael Molina, and Aggelos K Katsaggelos, "Using deep neural networks for inverse problems in imaging: beyond analytical methods," *IEEE Signal Processing Magazine*, vol. 35, no. 1, pp. 20–36, 2018.

[9] Qiangqiang Yuan, Huanfeng Shen, Tongwen Li, Zhiwei Li, Shuwen Li, Yun Jiang, Hongzhang Xu, Weiwei Tan, Qianqian Yang, Jiwen Wang, Jianhao Gao, and Liangpei Zhang, "Deep learning in environmental remote sensing: Achievements and challenges," *Remote Sensing of Environment*, vol. 241, pp. 111716, 2020.

[10] Aurélien Colin, Ronan Fablet, Pierre Tandeo, Romain Husson, Charles Peureux, Nicolas Longépé, and Alexis Mouche, "Semantic segmentation of metoceanic processes using SAR observations and deep learning," *Remote Sensing*, vol. 14, no. 4, 2022.

[11] Brandon Quach, Yannik Glaser, Justin Edward Stopa, Alexis Aurélien Mouche, and Peter Sadowski, "Deep learning for predicting significant wave height from synthetic aperture radar," *IEEE Transactions on Geoscience and Remote Sensing*, vol. 59, no. 3, pp. 1859–1867, 2020.

[12] Fabrice Collard, Fabrice Ardhuin, and Bertrand Chapron, "Extraction of coastal ocean wave fields from SAR images," *IEEE Journal of Oceanic Engineering*, vol. 30, no. 3, pp. 526–533, 2005.

[13] Xiao Xiang Zhu, Sina Montazeri, Mohsin Ali, Yuansheng Hua, Yuanyuan Wang, Lichao Mou, Yilei Shi, Feng Xu, and Richard Bamler, "Deep learning meets SAR: Concepts, models, pitfalls, and perspectives," *IEEE Geoscience and Remote Sensing Magazine*, vol. 9, no. 4, pp. 143–172, 2021.

[14] Klaus Hasselmann and Susanne Hasselmann, "On the nonlinear mapping of an ocean wave spectrum into a synthetic aperture radar image spectrum and its inversion," *Journal of Geophysical Research: Oceans*, vol. 96, no. C6, pp. 10713–10729, 1991.

[15] G. Engen, P.W. Vachon, H. Johnsen, and F.W. Dobson, "Retrieval of ocean wave spectra and rar mtf's from dual-polarization SAR data," *IEEE Transactions on Geoscience and Remote Sensing*, vol. 38, no. 1, pp. 391–403, 2000.

[16] Olaf Ronneberger, Philipp Fischer, and Thomas Brox, "U-net: Convolutional networks for biomedical image segmentation," in *Medical Image Computing and Computer-Assisted Intervention–MICCAI 2015: 18th International Conference, Munich, Germany, October 5-9, 2015, Proceedings, Part III 18*. Springer, 2015, pp. 234–241.

[17] Steven Guan, Amir A. Khan, Siddhartha Sikdar, and Parag V. Chitnis, "Fully dense unet for 2-d sparse photoacoustic tomography artifact removal," *IEEE Journal of Biomedical and Health Informatics*, vol. 24, no. 2, pp. 568–576, 2020.

[18] Kyong Hwan Jin, Michael T McCann, Emmanuel Froustey, and Michael Unser, "Deep convolutional neural network for inverse problems in imaging," *IEEE transactions on image processing*, vol. 26, no. 9, pp. 4509–4522, 2017.

[19] Romain Husson and Pauline Vincent, *Sentinel-1 Ocean Swell Wave Spectra (OSW) Algorithm Definition*, CLS,ESA, 2022.